

Corrigendum

Corrigendum to ‘Understanding and modelling wear rates and mechanisms in fretting via the concept of rate-determining processes - contact oxygenation, debris formation and debris ejection’

[Wear 486-487 (2021) 204066]

P.H. Shipway, A.M. Kirk, C.J. Bennett, T. Zhu
Faculty of Engineering, University of Nottingham, UK

The authors regret that we made an error in the equation proposed to describe one of the key processes in fretting, and would like to apologise for any inconvenience caused. The error relates to the equation proposed to describe the transport of oxygen to the active surface to form oxide debris. The main proposal and argument of the paper (namely that of the concept of rate-determining processes in fretting) is not affected by this error. Indeed, in the original paper itself (as highlighted in the abstract), we said:

“A number of assumptions have been made in deriving the equations which describe the key processes and it is recognised that these equations themselves may be refined in light of future research; however, any such revised equations can simply replace those proposed as part of the rate-determining process framework.”

1 The error and its implications

1.1 Basic summary of the original paper

A new framework which describes the role of three key processes in fretting wear of metals was proposed, with these three processes being: (i) oxygen transport into the contact; (ii) formation of oxide-based wear debris in the contact and (iii) ejection of the wear debris from the contact. To maintain system equilibrium in steady-state fretting, it was argued that these three processes must operate at the same rate as each other (debris cannot be ejected from the contact faster than it is formed, and debris cannot be formed faster than it is ejected). Accordingly, the *observed wear rate* is the rate of the process with the lowest rate of the three processes, with this process being termed the *rate-determining process* (RDP).

It is noted that two of the three key processes can be classified as transport processes (i.e. transport of oxygen into the contact to form oxide debris and transport of that debris out of the contact). In our paper, it was proposed that the rates of both transport processes decrease with increasing contact size (i.e. the distance over which transport of the species takes place). There is no general expectation that the dependence of these two rates upon the contact width will be the same and a generalised schematic diagram (Figure 5) was proposed in the original paper to describe this; this key figure is reproduced here in this corrigendum for clarity¹. It is noted that this is a schematic diagram and is therefore not affected by the error made in the derivation of the equation to describe one of these transport processes. Furthermore, it is argued that the RDP concept proposed is applicable to all fretting contacts, irrespective of

¹ Throughout this corrigendum, we have used the same figure numbers as in the original paper to aid comparison.

whether the contact is conforming or non-conforming, and irrespective of its dimensions and the direction of the fretting motion with respect to those dimensions.

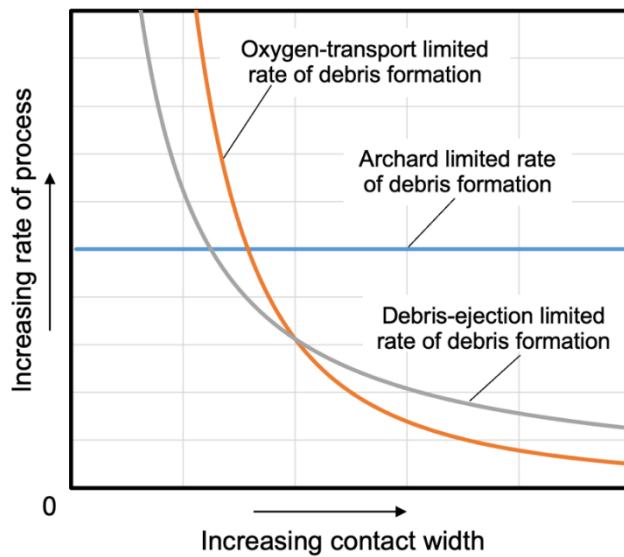


Figure 5 This figure reproduces that in the original paper with no change.

Schematic diagram illustrating the variations in the three rates as a function of contact width. The operative process at any contact width is that with the lowest of the three rates, with the observed rate being the rate of the operative process (RDP). Whilst this relates to both conforming and non-conforming contacts, it is noted that in the case of non-conforming contacts, the contact width increases as wear proceeds and accordingly there may be changes in the RDP throughout the exposure.

1.2 Nature of the error in the paper

A key assumption in the original paper is that the instantaneous rate of surface recession (wear), summed over the two specimens in the fretting pair, must be the same at all positions within the wear scar at any point in time. It was then argued that this means that the rate of consumption of oxygen required for formation of oxide debris, \dot{m} , will be the same at every point in the contact at a given time. It is noted that \dot{m} is defined as the consumption rate of oxygen per unit area of contact in the formation of oxide-based debris (with S.I. units of $\text{kg m}^{-2} \text{s}^{-1}$).

The error made in the original paper relates to the derivation of the rate equation related to oxygen transport into the contact to form oxide-based wear debris. In the formulation of Equation A1.8 in Appendix 1 of the original paper, we proposed that the total rate of consumption of oxygen required for debris formation across the whole contact will be directly proportional to the observed time-based rate of wear in the contact. We stand by this proposition; however, we made in an error in the way that this concept was formulated into an equation (we misinterpreted \dot{m} as being the rate of consumption of oxygen across the whole contact rather than the rate of consumption of oxygen per unit area across the whole contact). The **total** consumption rate of oxygen across the whole contact (as required in Equation A1.8) should have been given by the product of \dot{m} and the area of the contact at that point in time, $2 b L$ (where b is the contact semi-width and L is the contact length). Thus, the corrected form of equation A1.8 is formulated as follows:

$$2 b L \dot{m} = A' \frac{dV}{dt} \quad \text{Equation A1.8}$$

where A' is a constant with S.I. units of kg m^{-3} and $\frac{dV}{dt}$ is the time-based rate of wear.

This then leads to corrections being made in Equations A1.11 and A1.12, with the corrected form of Equation A1.12 (which forms a key basis-equation for the paper) being as follows:

$$\left(\frac{dV}{dE}\right)_{ot}^{max} = B' \frac{L C_{atm} D}{\delta^* \mu P f b} \quad \text{Equation A1.12}$$

where $\left(\frac{dV}{dE}\right)_{ot}^{max}$ is the maximum wear rate which can be sustained when controlled by the rate of oxygen transport into the contact, B' is a constant, C_{atm} is the atmospheric concentration of oxygen, D is the appropriate diffusion coefficient for transport of oxygen through the interface zone, δ^* is the displacement amplitude, μ is the coefficient of friction, P is the applied load and f is the fretting frequency.

It is noted that this proposal for the oxygen-transport limited rate of debris formation is based upon a number of physically reasonable assumptions, but that the paper does not claim that this is necessarily the correct form of the equation; indeed, as noted earlier, we expect these proposals to be refined in the course of subsequent research. With that caveat in mind, the reader will note that in the original (erroneous) version of Equation A1.12, the oxygen-transport limited rate of debris formation, $\left(\frac{dV}{dE}\right)_{ot}^{max}$ is proportional to $1/b^2$, but in the corrected version, it is instead proportional to $1/b$. This dependence upon b (under our current set of assumptions) happens to be the same as the dependence of the debris-ejection limited rate of debris formation upon b , and therefore, the transition between debris expulsion from the contact and oxygen supply to form debris being rate-determining (as illustrated for the general case in Figure 5 from the original paper) will never occur. [We do note that as equations are refined in future, this transition between which processes are rate determining may be seen again depending upon the exact form of the equations].

1.3 Locations of the corrected equation in the paper, and replacement of derived constants

It is noted that the incorrect equation derived in Appendix 1 was reproduced elsewhere in the paper, and therefore also needs to be corrected in these locations (namely in Equation 2 and Table 1). Specifically, Equation 2 in the original paper should also be re-written as follows:

$$\left(\frac{dV}{dE}\right)_{ot}^{max} = B' \frac{L C_{atm} D}{\delta^* \mu P f b} \quad \text{Equation 2}$$

It is noted that each of the key equations required tuning against experimental data, with the *oxygen transport constant* ($B' \times D$) being calculated as described in Section 3.3. The correction of Equation 2 also requires that the oxygen transport constant needs to be recalculated. The new value oxygen transport constant ($B' \times D$) of $13.75 \times 10^{-15} m^3 s^{-1} (kg_{O_2} m^{-3})^{-1}$ was derived by fitting against the same experimental data as described in the original paper. It is noted that the units of the oxygen transport constant ($B' \times D$) have also been corrected in light of the new form of Equation 2. For the sake of clarity, a corrected form of Table 1 from the original paper reproduced here:

Table 1 There are changes to this table from that in the original paper as a result of the corrections made.

Summary of the competing rate equations (as described in Sections 2.2 – 2.4 of the original paper) and the evaluated and defined constants.

Physical process	Equation	Constants	Value employed in the model
Archard wear (section 2.2)	$\left(\frac{dV}{dE}\right)_{Arch}^{max} = A$	A	$90 \times 10^{-15} m^3 J^{-1}$
Oxygen transport (section 2.3)	$\left(\frac{dV}{dE}\right)_{ot}^{max} = B' \frac{L C_{atm} D}{\delta^* \mu P f b}$	$(B' \times D)$	$13.75 \times 10^{-15} m^3 s^{-1} (kg_{O_2} m^{-3})^{-1}$
		C_{atm}	$0.3 kg_{O_2} m^{-3}$
Debris ejection (section 2.4)	$\left(\frac{dV}{dE}\right)_{de}^{max} = \frac{G \beta}{\mu b}$	$(G \times \beta)$	$23.6 \times 10^{-18} m^4 J^{-1}$

1.4 Implications of correction of the error

A key finding in the original paper is that when the oxygen-transport limited rate of debris formation is rate-determining, significant sub-surface damage was observed in cross-sections through the wear scars, with it being proposed that this was due to oxygen starvation in the contact meaning that a protective debris bed was not able to form, resulting in metal-metal contact. To enable the implications of the corrections to be clearly described, Figure 12 from the original paper is presented below, with the conditions under which sub-surface damage was and was not observed being clearly indicated.

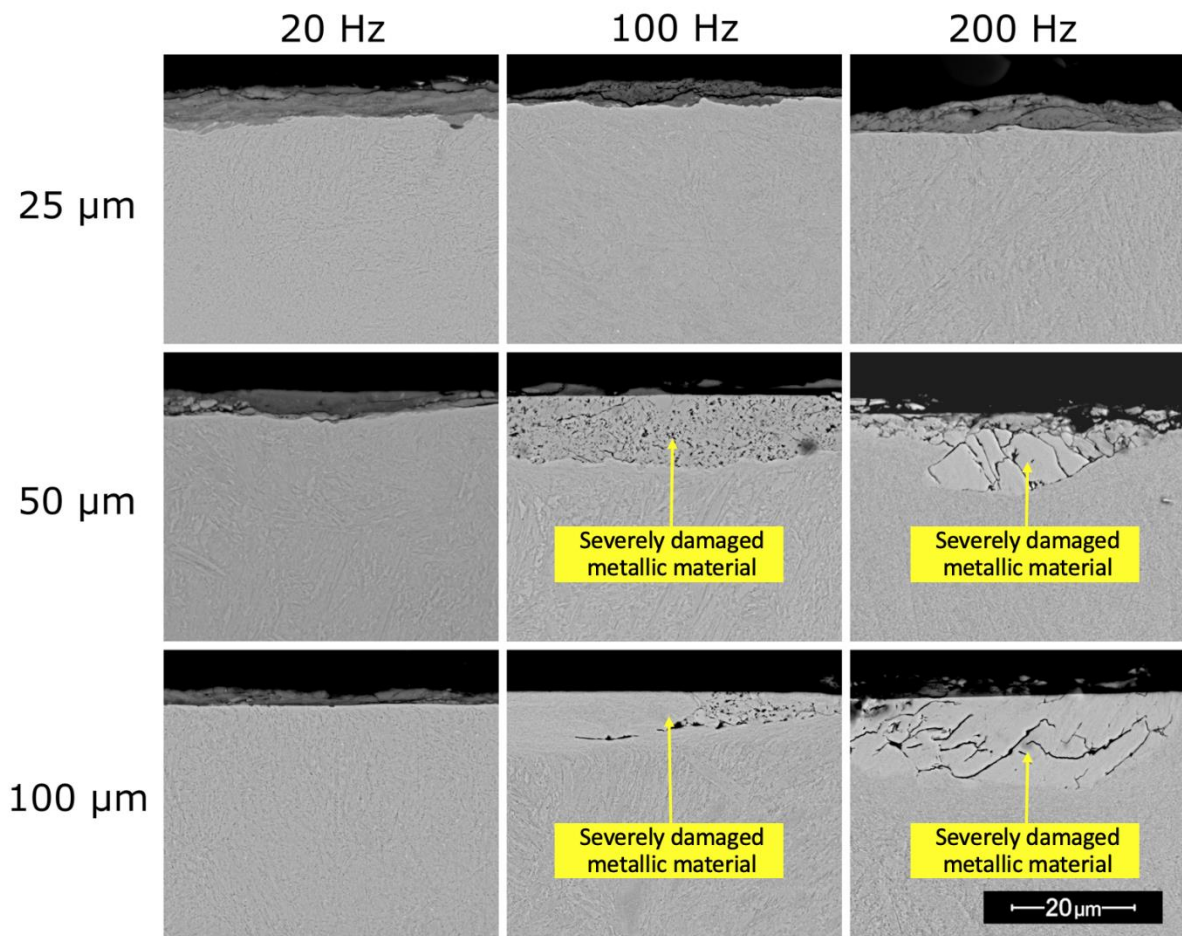


Figure 12 This figure reproduces that in the original paper with no change.

BSE SEM micrographs in sectional view of cylinder specimens after fretting for 10^6 cycles over the range of frequencies and applied displacement amplitudes examined, showing the development of significant levels of subsurface damage associated with increases in both parameters [1]. Fretting direction is left ↔ right in all cases.

Figure 14 from the original paper is re-presented here, with the oxygen-transport limited rate of debris formation (orange line) now being illustrated in accord with the corrected form of Equation 2. Comparison of the corrected version of Figure 14 and the micrographs shown in Figure 12 indicate that the original proposition (namely that oxygen-transport limited rate of debris formation being rate-determining results in sub-surface damage) is still valid.

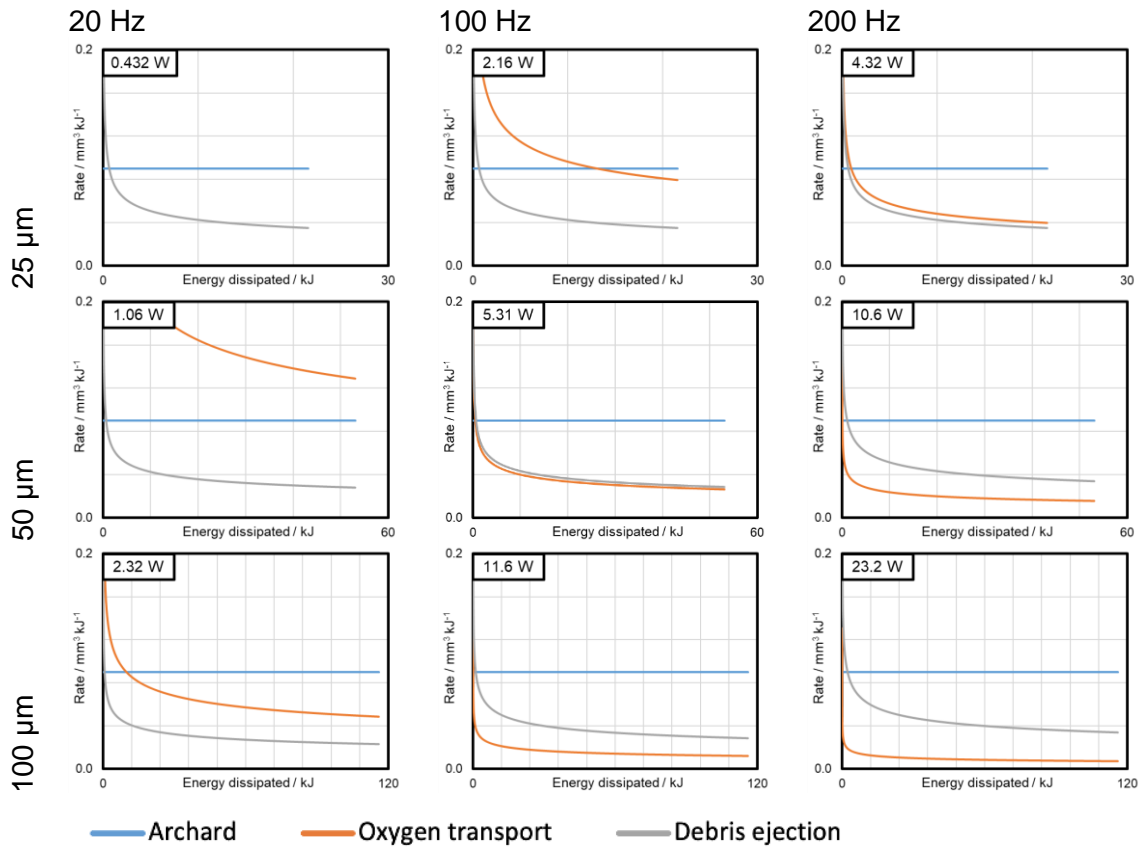


Figure 14 There are changes to this table from that in the original paper as a result of the corrections made.

Evolution of RDPs (indicated by the process with the lowest rate at any point during a test) over the range of displacement amplitudes and frequencies studied experimentally [1]. Gridlines are spaced by 10 kJ in each of the graphs, highlighting the difference in total dissipated energy associated with changes in displacement amplitude ($P = 450 \text{ N}$; $N = 10^6$ cycles; $L = 10 \text{ mm}$). In each case, the frictional power dissipated (calculated using the assumptions made for the modelling work) is indicated.

All the figures and tables which are presented after Figure 14 in the original paper are to some degree affected by the correction of Equation 2. However, the principles behind their derivation remain valid; moreover, the original paper was not based upon experimental work, with these data from the literature simply being used to illustrate the application of the proposed framework. Notwithstanding, a number of the figures and tables from the original paper which have been affected by the correction made to Equation 2 are now reproduced in their corrected form, and a commentary made in each case.

Figure 15 in the original paper was included to clarify the impact of displacement amplitude on the relative rates of processes and showed the observed wear rate at any given point in a test (i.e. the rate of the RDP as shown in Figure 14) plotted on the same scale for all three displacement amplitudes at each frequency. The correction of the error has resulted in slight changes in the rates, but the trends remain unchanged at all three frequencies (complete overlay of the rates associated with the three displacement amplitudes at the lowest frequency (20 Hz) with increased separation between the rates associated with the different displacement amplitudes at higher frequencies). To illustrate the magnitude of the changes, a revised version of Figure 15c is presented here; when compared with that in the original paper,

it can be seen that the correction does not result in a significant difference, with the broad trends being unchanged.

Figure 16 in the original paper was included to show a comparison between measured wear volumes from an experimental paper and the associated predictions from the model. As in the original paper, the correlation between the experimental data and the corrected model predictions remains reasonable (but not strong). Again, the broad trends are not changed by the corrections made in this corrigendum.

Figure 17 in the original paper was an illustrative example of the predicted evolution of wear volume with energy dissipated throughout tests with 1×10^6 fretting cycles and a fretting frequency of 100 Hz, but with different displacement amplitudes. The corrected form of Figure 17 illustrates that correction to Equation 2 in this corrigendum has not resulted in a significant difference with the broad trends being unchanged.

In the original paper, the contributions of wear under the different RDPs to the total wear in a test were presented in Figure 18. The corrected form of Equation 2 means that (with the assumptions under which these were derived), both the debris-ejection limited rate of debris formation and the oxygen-transport limited rate of debris formation have the same dependence on the contact width, b (both being proportional to $1/b$) so that as the test proceeds (and thus b increases in size due to the non-conforming nature of the contact), there is never any switch between the debris-ejection and oxygen-transport limited rates being rate-determining. As such, in each case in the corrected form of Figure 18 shown here, there is a small blue line (representing the initial Archard-controlled wear) followed by either wear under debris-ejection control (a grey bar) or wear under oxygen transport control (an orange bar).

In the original paper, Table 2 sought to illustrate schematically the expected influence of a particular test parameter on the overall wear volume observed in a test depending upon the operative RDP, whilst Table 3 sought to illustrate schematically how the magnitude of each parameter broadly influences which process is rate-determining. The correction of Equation 2 has resulted in some small changes to each of these tables associated with the dependence upon and the influence of the contact width, b .

2 Summary and conclusions

We apologise for the error made in the original work and for any confusion that may have resulted from this. However, the basic framework and approach outlined originally is not affected by the error made, and the robustness of the approach is demonstrated through this corrigendum. Moreover, it is highlighted that subsequent changes to the basic equations in light of future research insights (e.g. associated with the role of specific fretting parameters or contact geometries) do not affect the basic framework and approach. We recognise that correction of this error has resulted in changes in much of the illustrative work in the paper, but do note that the magnitude of changes are often small and that the trends and correlations described originally are still supported; of note amongst these is the strong correlation between the observation of extensive sub-surface damage in a wear scar and oxygen-transport limited rate of debris formation being the rate-determining process (RDP).

3 References

[1] A.M. Kirk, W. Sun, C.J. Bennett, P.H. Shipway, Interaction of displacement amplitude and frequency effects in fretting wear of a high strength steel: impact on debris bed formation and subsurface damage, *Wear*. 482–483 (2021). <https://doi.org/10.1016/j.wear.2021.203981>.

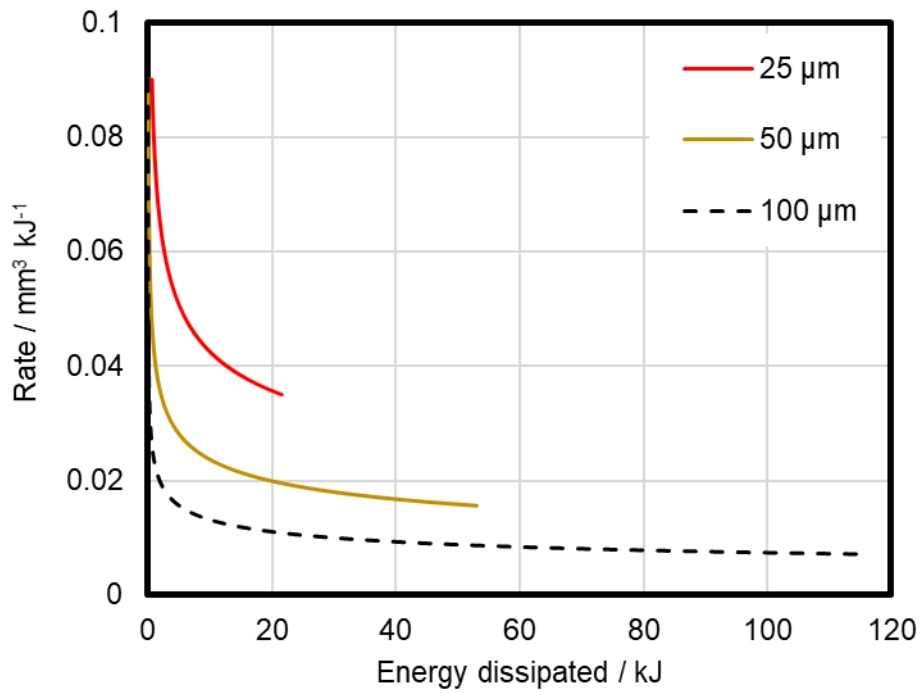


Figure 15 (c) There are changes to this figure from that in the original paper as a result of the corrections made.

Observed wear rate (i.e. the rate of the RDP at a given dissipated energy) across the range of displacement amplitudes examined at a fretting frequency of 200 Hz ($P = 450$ N; $N = 10^6$ cycles; $R = 6$ mm; $L = 10$ mm).

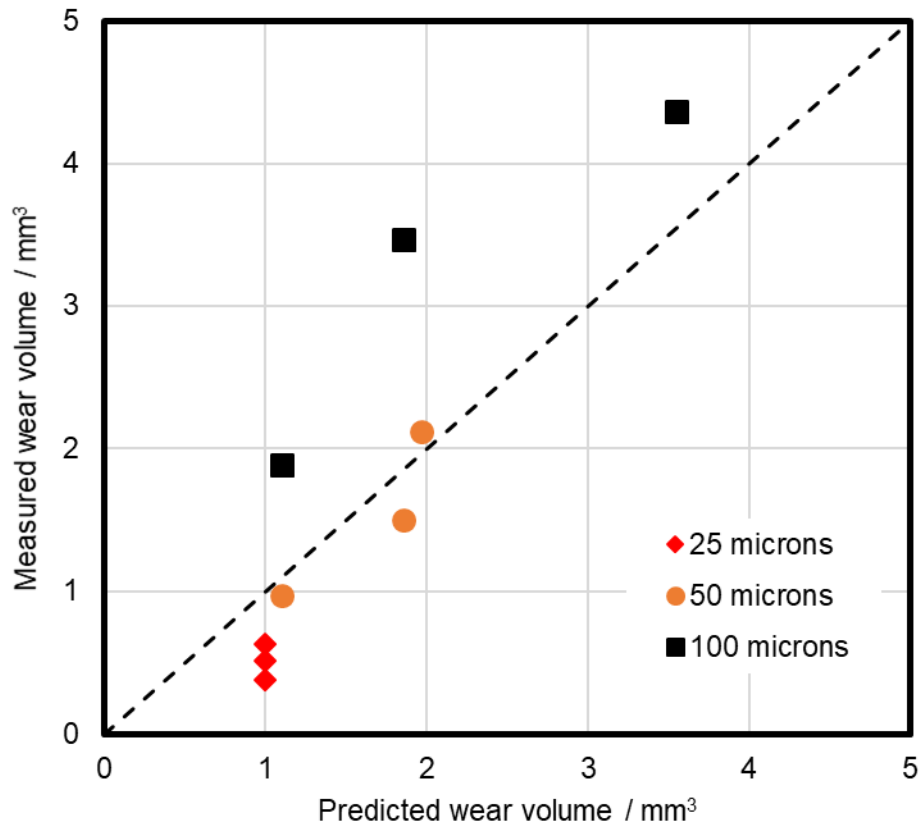


Figure 16 There are changes to this figure from that in the original paper as a result of the corrections made.

Comparison of predicted and measured wear volumes for the experimental data from the literature [1] with the line of equality marked.

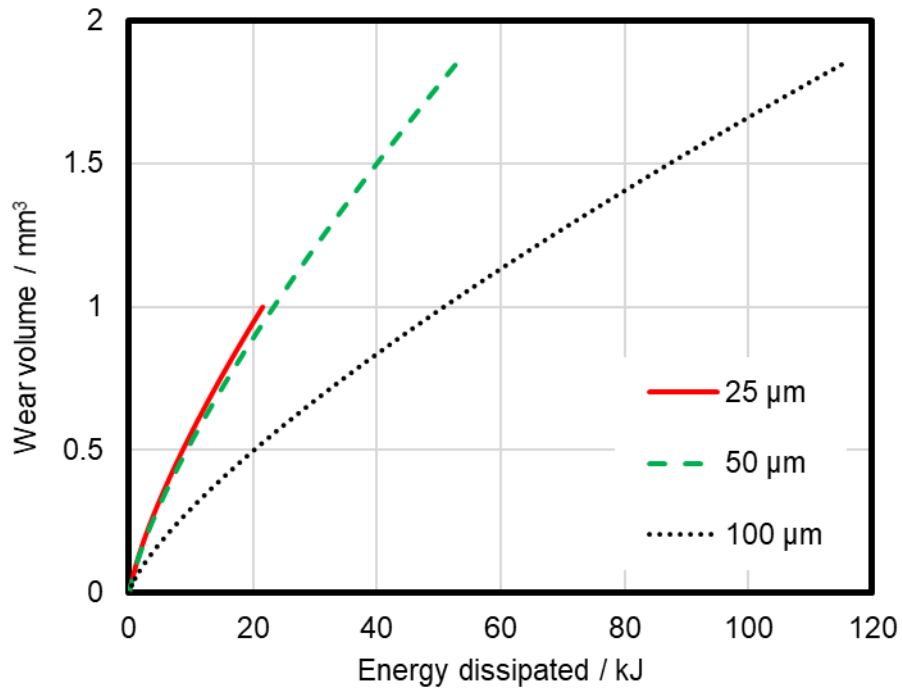
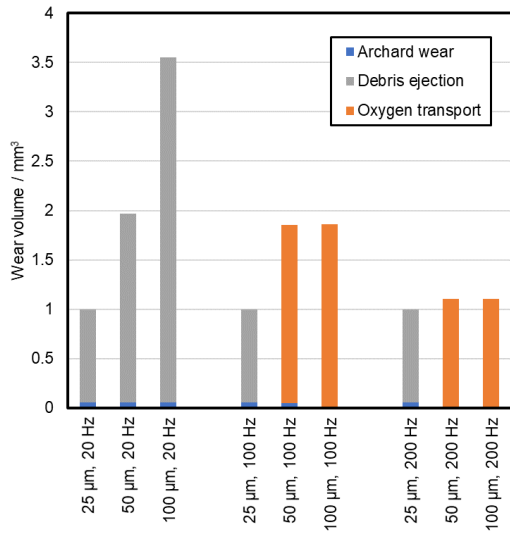
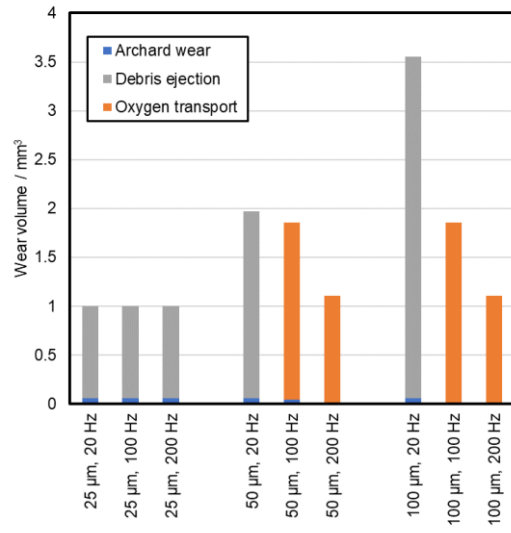


Figure 17 There are changes to this figure from that in the original paper as a result of the corrections made.

Evolution of predicted wear volume with increasing dissipated energy over a range of applied displacement amplitudes with fretting frequency of 100 Hz. Model conditions replicate those employed in generation of the experimental data presented in Figure 16.



(a)



(b)

Figure 18 There are changes to this figure from that in the original paper as a result of the corrections made.

Predicted wear volumes for the different test conditions considered in the work behind the data presented in Figure 16 (displacement amplitude and fretting frequency were varied whilst number of cycles and applied load were kept constant): (a) grouped by test frequency; (b) grouped by displacement amplitude. In each case, the total wear volume is sub-divided to show the fractions generated under the control of the three potential RDPs.

Table 2 There are changes to this table from that in the original paper as a result of the corrections made.

Predictions of the effect of change in various parameters on the observed wear rate depending upon the operative RDP. This information is a graphical representation of that contained in the equations presented in Table 1.

Change in test parameter	Effect on parameter change on rate depending upon operative RDP		
	Archard wear	Oxygen transport	Debris ejection
b ↑	—	↓	↓
C_{atm} ↑	—	↑	—
δ^* ↑	—	↓	—
μ ↑	—	↓	↓
P ↑	—	↓	—
f ↑	—	↓	—

Table 3 There are changes to this table from that in the original paper as a result of the corrections made.

Effect of changes in governing parameters on the operative RDP

Parameter	Tendency in operative RDP with increase in parameter		
b	Archard	→	Debris ejection Oxygen transport
C_{atm}	Oxygen transport	→	Archard Debris ejection
δ^*	Archard Debris ejection	→	Oxygen transport
μ	Archard	→	Debris ejection Oxygen transport
P	Archard Debris ejection	→	Oxygen transport
f	Archard Debris ejection	→	Oxygen transport
L	Oxygen transport	→	Archard Debris ejection